Superlattice Electronic Devices as Millimeter-Wave Sources

Heribert Eisele [*], Suraj P. Khanna, and Edmund H. Linfield
Institute of Microwaves and Photonics, School of Electronic and Electrical Engineering
University of Leeds, Leeds LS2 9JT, United Kingdom
[*] Email: h.eisele@leeds.ac.uk

Abstract: Negative differential resistance devices were fabricated from four epitaxial wafers with different GaAs/AlAs superlattices and evaluated in resonant-cap full-height WR-15 and WR-10 waveguide cavities. These devices on integral heat sinks generated output powers in the fundamental mode between $62–108 GHz$. The best RF powers (and their corresponding dc-to-RF conversion efficiencies) were $58 mW$ (3.5%) at $66 GHz$, $42 mW$ (2.6%) at $78 GHz$, and $28 mW$ (1.8%) at $94 GHz$. The RF power of $15 mW$ at $101 GHz$ constitutes a 30-fold improvement over previous results; the highest fundamental oscillation frequency was $108 GHz$. In a second-harmonic mode, one device yielded $2.0 mW$ at $216 GHz$, the highest second-harmonic frequency to date for a GaAs/AlAs superlattice.

Keywords: Harmonic operation, Millimeter-wave oscillator, Negative differential resistance device, Spectral purity, Superlattice

1. Introduction

Compact, reliable, and efficient sources of radiation are a prerequisite for many emerging systems applications at terahertz frequencies, such as wideband wireless communications, material analysis, imaging, chemical and biological sensing, and space exploration. High spectral purity is also imperative for these sources to be used as transmitters or local oscillators in such applications [1]. In their seminal paper of 1970, Esaki and Tsu proposed a device structure "with virtually no frequency limitation" where the Bragg reflection of electrons in an engineered semiconductor superlattice (SL) gives rise to energy minibands and regions of negative differential velocity [2] in the velocity-electric field characteristics. At sufficiently high electric fields across a doped SL, traveling domains may then form in the SL [3] and, similar to domains in Gunn devices, cause a negative differential resistance (NDR) to occur between the device terminals. When a superlattice electronic device (SLED) with such an NDR is connected to a suitable resonant RF circuit, RF power is generated.

SLEDs have attracted much attention since the 1990s because the underlying physical process, the Bloch effect, has relevant time constants that are much shorter than those of the transferred-electron effect in, for example, GaAs Gunn devices [4]. SLEDs with sufficiently wide minibands in the GaAs/AlAs and InGaAs/InAlAs material systems have been demonstrated as millimeter-wave oscillators [4-7]. As examples, fundamental-mode operation up to $103 GHz$ (with an RF output power of $0.5 mW$) was demonstrated for a GaAs/AlAs SL [4], and a high dc-to-RF conversion efficiency of 5% at $64.4 GHz$ was obtained with a SLED in a cavity micromachined using SU-8 [7]. More recently, the use of selective etching technologies [8], and improved thermal management with substrateless devices, yielded RF output powers of more than $80 mW$ and dc-to-RF conversion efficiencies up to 5.1% around $63 GHz$ [9]. This paper reports the demonstration of SLEDs as high-performance millimeter-wave oscillators above $75 GHz$.

2. Experimental Procedure

Four different SL structures were grown in an Oxford Instruments (VG Semicon) V80-H molecular beam epitaxy growth chamber at a substrate temperature of 580°C and with a V/III flux ratio of approximately 7. In this MBE system, the substrate temperature is determined using a k-Space Associates calibrated BandiT spectrometer, whereas the flux ratio is determined by a beam monitoring ion gauge. The growth conditions for the four wafers were similar to those used at the time to grow high electron mobility transistor structures with mobilities exceeding $106 cm \cdot V\text{-}1 s\text{-}1$ at 1.2K. Doping levels were assessed by growing separate bulk GaAs layers for Hall effect measurements.

Tab.1 lists the structural properties of the four wafers and their estimated miniband widths [11]. To increase the operating frequency slightly from previously evaluated devices [9], the total lengths of these SL structures were reduced for Wafers 2-4 by approximately 12-15%, and for Wafer 4, a wider miniband width was also chosen. In all four wafers, and as before [9], the SLs were sandwiched between graded transition layers and thin buffer layers on both sides. A 0.5-μm-thick Al0.55Ga0.45As layer was grown between the substrate and the SLED layers to allow for complete substrate removal during device fabrication [8].

Wafer	Number of periods	Number of GaAs MLs	Number of AlAs MLs	Nominal doping [cm^{-3}]	Miniband width [meV]
1	120	12	3	1.5×10^{17}	85
2	102	12	3	1.6×10^{17}	85
3	102	12	3	1.9×10^{17}	85
4	110	12	2	1.5×10^{17}	150

Tab. 1 Nominal device structures of the wafers used for millimeter-wave superlattice electronic devices.

Device fabrication followed the same process steps described in [9] except that the top ohmic contacts were defined by etching in a wet etchant [12] for all fabrication runs, and somewhat smaller SLEDs, with nominal diameters of 30-55μm, were selected for packaging and RF testing. SLEDs were mounted in the same type of package that has been employed previously in the evaluation of different types of active two-terminal devices on integral and diamond heat sinks in the GaAs and InP material systems [8], including SLEDs [9].

SLEDs fabricated from each of the four wafers were evaluated in the fundamental mode and in higher harmonic modes. For fundamental-mode operation, the same types of resonant-cap full-height WR-15 and WR-10 waveguide cavities were employed, as previously used in the evaluation of various two-terminal devices in the GaAs and InP material systems at V-band (50-75GHz) frequencies [8], and W-band (75-110GHz) frequencies [8], respectively. RF output powers and oscillation frequencies were measured in calibrated WR-15 (V-band) and WR-10 (W-band) waveguide test setups that each have a precision attenuator, a precision direct-reading frequency meter, a thermistor power head, and a directional coupler to connect to a harmonic

mixer [8].

For operation in a second-harmonic mode below approximately 190GHz, the SLEDs had to be mounted in a different package, which fitted the highly tunable waveguide mount of Fig.1. This mount previously yielded state-of-the-art results from InP Gunn devices above 180GHz [14] and SLEDs around 130GHz [9]. Therefore, the SLEDs for this mount were not evaluated in the fundamental mode. Conversely, the SLEDs with fundamental oscillation frequencies above 100GHz were also evaluated for second-harmonic power extraction, and the waveguide configuration of Fig.2 was employed. It is one of the configurations that were used previously for the same purpose with GaAs tunnel injection transit-time (TUNNETT) diodes [14].
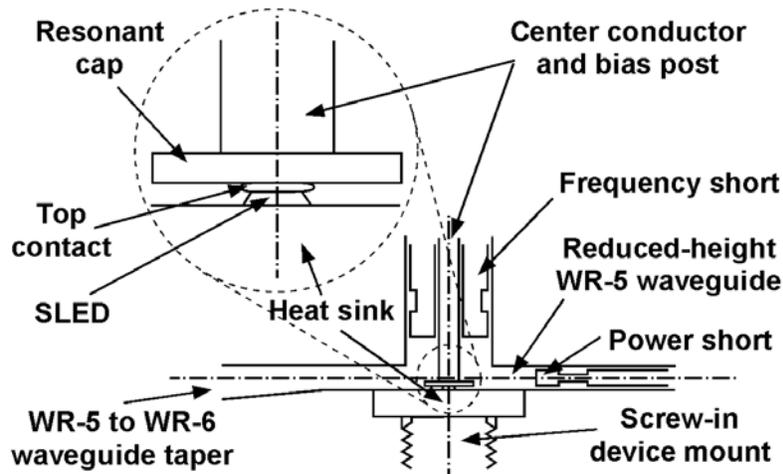
Fig.1 Schematic of the waveguide oscillator mount for second-harmonic power extraction from SLEDs from Wafers 1-3 below 190GHz.
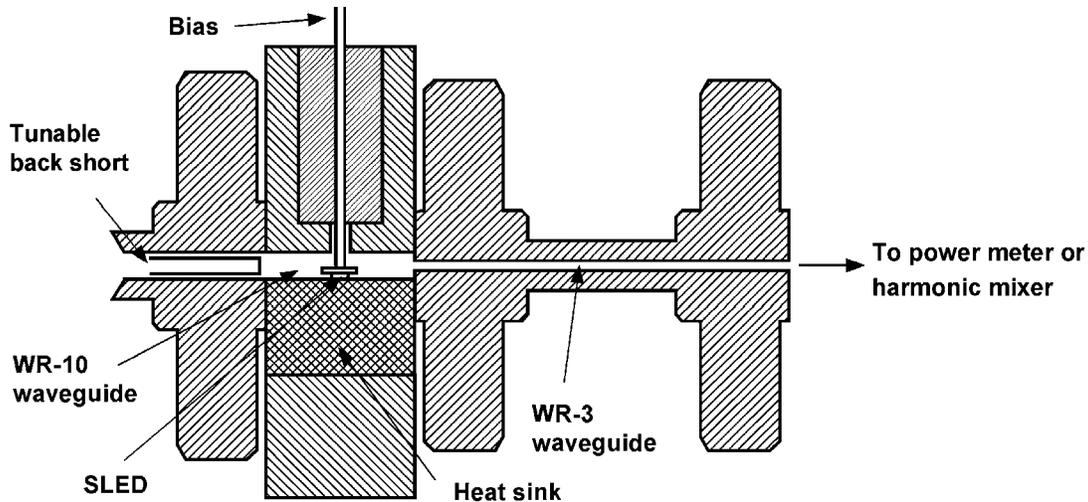
Fig.2 Schematic of the WR-10 waveguide oscillator cavity and WR-3 output waveguide for second-harmonic power extraction from SLEDs from Wafer 4.

3. Results

The current-voltage characteristics of SLEDs from Wafers 1-4 are very similar to that reported previously [9] and typically show the onset of a negative slope at a dc bias voltage of approximately $0.8V$. SLEDs from Wafer 1 yielded RF powers (and corresponding dc-to-RF conversion efficiencies) of $52mW$ (4%) and $58mW$ (3.5%) at $62.7GHz$ and $66.4GHz$, respectively, and these values are comparable to those typical for the SLEDs of [9]. In a second-harmonic mode, one SLED from Wafer 1 generated an RF power of $5mW$ around $150GHz$ in the mount of Fig.1.

Contrary to the SLEDs of [9] however, SLEDs from Wafer 1 could be operated easily in a WR-10 waveguide cavity and at fundamental frequencies above $75GHz$. They then produced RF powers of $31mW$ and $20mW$ at $75.2GHz$ and $87.1GHz$, respectively. RF powers of 20-$25mW$ around $75GHz$ were measured with SLEDs from Wafer 2 in a WR-15 waveguide cavity whereas SLEDs from Wafer 3 yielded much higher RF powers (and corresponding dc-to-RF conversion efficiencies) of $47mW$ (3%) at $66.6GHz$ and $42mW$ (2.6%) at $77.8GHz$ in the same cavity.

The spectral purity of the fundamental-mode oscillations in V-band was verified with an Agilent E4407B spectrum analyzer and an Agilent 11970V waveguide harmonic mixer connected to the V-band waveguide setup. Typical dc bias voltages of the SLEDs from the four wafers are below 3V. At such bias voltages, even small noise signals (less than $1mV$) from the power supply were found to cause appreciable frequency modulation and broadening of the line width of the oscillators. As a consequence, the same bias filter as for the 480-GHz oscillator with an InP Gunn device [16], consisting of a series resistor of 1Ω and a parallel capacitor of more than $50mF$, was connected between the power supply and the SLED under test. The spectral purity of the SLEDs was found to be as good as or better than that reported in [9].

The SLEDs from Wafer 4 were first tested in a WR-10 waveguide cavity and instantly achieved the highest oscillation frequencies of the four wafers of Tab. . Therefore, they were not tested in a WR-15 waveguide cavity. The best results to date are RF powers (and corresponding dc-to-RF-conversion efficiencies) of $28mW$ (1.8%) at $94.5GHz$ and $15mW$ (1.0%) at $101.0GHz$.

The employed WR-15 and WR-10 waveguide cavities generally do not support the operation of devices in a second-harmonic mode at 50-$75GHz$ and 75-$110GHz$, respectively. Nonetheless, two types of additional experiments were carried out to confirm that the SLEDs from Wafer 4 were operating in the fundamental mode. The tunable back short in the waveguide greatly changes the impedance seen by the active two-terminal device and, consequently, its oscillation frequency when the device is operating in the fundamental mode. As a result, active two-terminal devices in the fundamental mode commonly show monotonic tuning behavior and a wide tuning range when the position of the back short is changed [8], Conversely, the oscillation frequency of an active two-terminal device in a second-harmonic mode is hardly affected by the tunable back short such as the power short in the waveguide of the mount of Fig.1.

As can be seen from Fig.3, the SLED from Wafer 4 can be tuned monotonically (and virtually linearly) by more than $6GHz$, that is, from $101.1GHz$ to $107.7GHz$, when the position of the back short is changed by $0.7mm$. No mode or frequency jumps occur over the full tuning range, and an RF output power of more than $11mW$ is available over a smaller tuning range, which still exceeds $4GHz$. Such a wide tuning range is a clear indication of operation in the fundamental mode.

SLEDs are well known to generate strong signals at higher harmonic frequencies [7],. Therefore, the same SLED whose tuning characteristics were presented in Fig.3 was also evaluated for its performance in the configuration of Fig.2. For different positions of the back short, RF powers of 2.2*mW* and 1.3 *mW* were measured at 207.7*GHz* and 212.3*GHz*, respectively and confirm again that the results presented in Fig.3 correspond to operation in the fundamental mode.
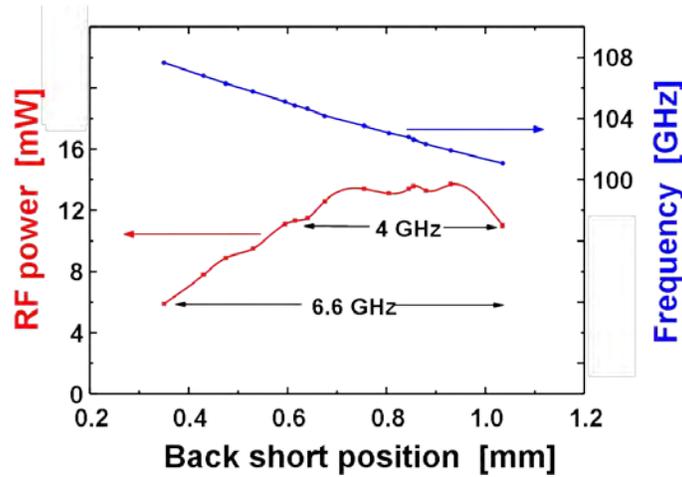
Fig.3 RF output power and oscillation frequency as a function of backshort position for a GaAs/AlAs SLED from Wafer 4 operating in the fundamental mode on an integral heat sink.
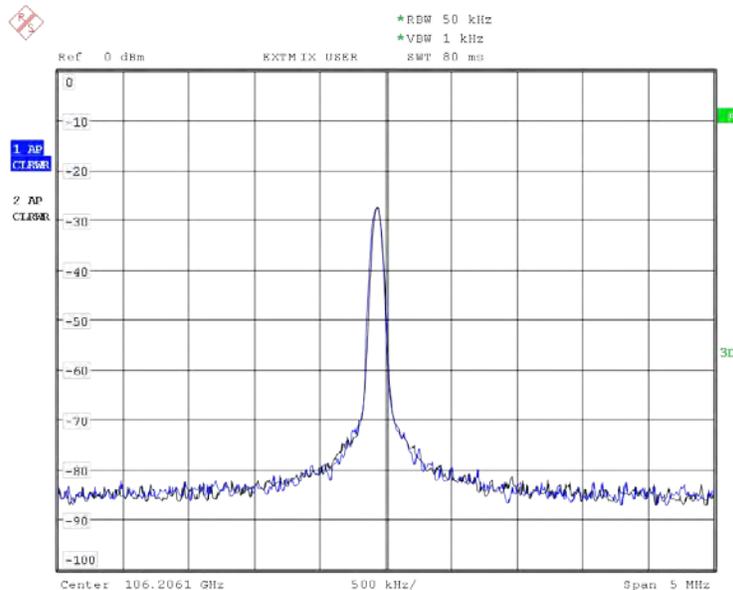
Fig.4 Spectrum of a free-running oscillator with a SLED from Wafer 4 in the fundamental mode; RF power: 8*mW*, center frequency: 106.21*GHz*, vertical scale: 10*dB/div*., horizontal scale: 500*kHz/div.,* resolution bandwidth: 50*kHz*, video bandwidth: 1*kHz*.

The excellent spectral purity of SLEDs from Wafer 4 at the fundamental and second-harmonic frequencies was ascertained using a Rohde & Schwarz FSU-46 spectrum analyzer either with a

W-band harmonic mixer connected to the WR-10 waveguide setup or a J-band (170-325*GHz*) mixer connected to the output waveguide of Fig.2. The same bias filter as before with a series resistor and a parallel capacitor [16] was used. Fig.4 shows the spectrum of the SLED for an RF power of 8*mW* at 106.2*GHz* and Fig.5 the spectrum of the same SLED for an RF power of 1.3*mW* at 212.3*GHz*. Both figures show the two traces that are produced by the IDENTIFY function of the spectrum analyzer.
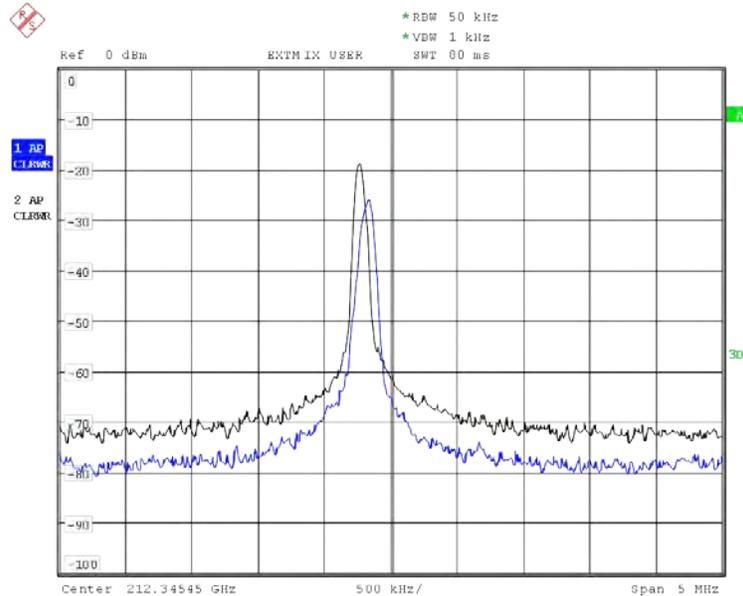
Fig.5 Spectrum of a free-running oscillator with a SLED from Wafer 4 in a second-harmonic mode; RF power: 1.3*mW*, center frequency: 212.34*GHz*, vertical scale: 10*dB/div*., horizontal scale: 500*kHz/div*., resolution bandwidth: 50*kHz*, video bandwidth: 1*kHz*.
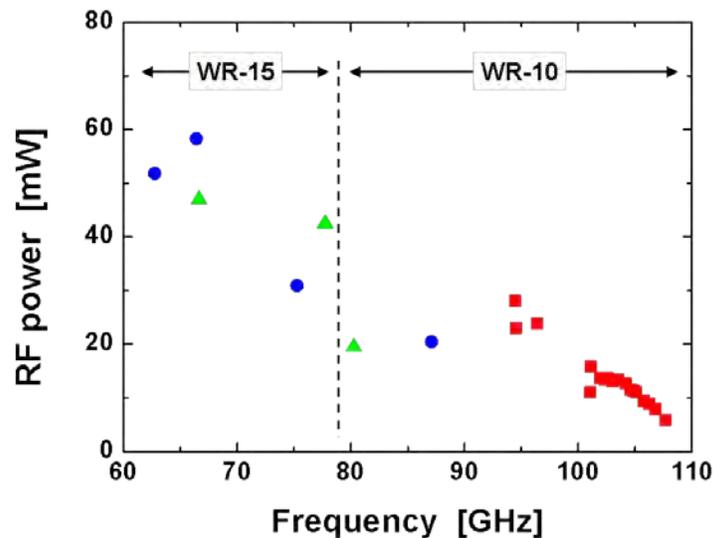
Fig.6 RF powers from SLEDs of Wafers 1(●), 3(▲) and 4(■) in the fundamental mode over the frequency range 60-110*GHz*.

The SLED of Fig. 3-5 Fig.3-Fig.5 was removed from its WR-10 cavity to allow for testing of

other SLEDs from Wafers 3 and 4. It was then tested again after reassembly with the same resonant cap as before and the aforementioned RF power of 15mW was measured at 101.0GHz. For the same resonant cap, but different positions of the tunable back short, it also yielded RF powers of 24mW at 96.4GHz in the fundamental mode and 2.0mW at 216.3GHz in a second-harmonic mode. Fig.6 summarizes the best results from Wafers 1, 3, and 4 of Tab.   in the fundamental mode over the frequency range 60-110GHz. The RF power of 15mW at 101.0GHz constitutes a 30-fold improvement over previous results [4] and this performance improvement confirms the importance of suitable thermal management in SLEDs [9], as already known from other active two-terminal devices [8]. Furthermore, RF powers of 2.2mW at 207.7GHz and 2.0mW at 216.3GHz are several orders of magnitude higher than those reported before. The oscillation frequency of 107.7GHz is the highest reported to date from GaAs/AlAs SLEDs operating in the fundamental mode and also much higher than the highest reported to date for GaAs Gunn devices operating in the fundamental mode (87GHz) [8].

4. Conclusions

The experimental results reported in this paper show that shorter SL structures and wider miniband widths lead to higher operating frequencies. They are also a very good indication of the strong potential of SLEDs as high-performance fundamental sources for millimeter-wave and submillimeter-wave frequencies up to 1THz. Further performance improvements are expected not only from fully optimized thermal management, but also from SL structures designed for higher operating frequencies or more efficient harmonic operation. In addition, approaches to efficient third-harmonic power extraction that have already been demonstrated with GaAs TUNNETT diodes [18] and InP Gunn devices up to 480GHz [16], [19] could be implemented.

Acknowledgment

References

[1]   P. Siegel, "Terahertz technology," *IEEE Trans. Microw. Theory Tech.*, 50(3), 910–928, (2002).

[2]   L. Esaki and R. Tsu, "Superlattice and negative differential conductivity in semiconductors," *IBM J. Res. Develop.*, 14(1), 61–65, (1970).

[3]   H. Le Person, C. Minot, L. Boni, J. F. Palmier, and F. Mollot, "Gunn oscillations up to 20 GHz optically induced in GaAs/AlAs superlattice," *Appl. Phys. Lett*, 60(19), 2397–2399, (1992).

[4]   E. Schomburg, M. Henini, J. M. Chamberlain, P. Steenson, S. Brandl, K. Hofbeck, K. F. Renk, and W. Wegscheider, "Self-sustained current oscillation above 100GHz in a GaAs/AlAs superlattice," *Appl. Phys. Lett.*, 74(15), 2179–2181, (1999).

[5] R. Scheuerer, E. Schomburg, K. F. Renk, A. Wacker and E. Schöll, "Feasibility of a semiconductor superlattice oscillator based on quenched domains for the generation of submillimeter waves," *Appl. Phys. Lett.*, 81(8), 1515–1517, (2002).

[6] E. Schomburg, R. Scheuerer, S. Brandl, K. F. Renk, D. G. Pavel'ev, Yu. Koschurinov, V. Ustinov, A. Zhukov, A. Kovsh, and P. S. Kop'ev, "An InGaAs/InAlAs superlattice oscillator at 147 GHz," *Electron. Lett.*, 35(17), 1491–1492, (1999).

[7] M. Häußler, E. Schomburg, J.-M. Batke, F. Klappenberger, A. Weber, H. Appel, K.F. Renk, H. Hummel, B. Ströbl, D.G. Pavel'ev and Yu. Koschurinov, "Millimetre-wave generation with semiconductor superlattice mounted in cavity fabricated by UV-photolithography and galvanoforming," *Electron. Lett.*, 39(10), 784–785, (2003).

[8] H. Eisele and G. I. Haddad, "Active Microwave Diodes," in *Modern Semiconductor Devices*, S. M. Sze, Ed., Ch. 6, John Wiley & Sons, New York, 343–407, (1997).

[9] H. Eisele, I. Farrer, E. H. Linfield, and D. A. Ritchie, "High-performance millimeter-wave superlattice electronic devices," *Appl. Phys. Lett.*, 93(18), 182105-1–182105-3, (2008).

[10] H. Eisele, S. P. Khanna, and E. H. Linfield, "Superlattice electronic devices as high-performance oscillators between 60–220 GHz," *Appl. Phys. Lett.*, 96(7), 072101-1–072101-3, (2010).

[11] G. Bastard, "Superlattice band structure in the envelope-function approximation," *Phys. Rev. B,* 24(10), 5693–5697, (1981).

[12] H. Eisele, "Selective etching technology for 94 GHz GaAs IMPATT diodes on diamond heat sinks," *Solid-State Electron.*, 32(3), 253–257, (1989).

[13] H. Eisele and G. I. Haddad, "Two-terminal millimeter-wave sources," *IEEE Trans. Microw. Theory Tech.*, 46(6), 739–746, (1998).

[14] H. Eisele, A. Rydberg, and G. I. Haddad, "Recent advances in the performance of InP Gunn devices and GaAs TUNNETT diodes for the 100–300-GHz frequency range and above," *IEEE Trans. Microw. Theory Tech.*,48(4), 626–631, (2000).

[15] H. Eisele and R. Kamoua, "Submillimeter-wave InP Gunn devices," *IEEE Trans. Microw. Theory Tech.*, 52(10), 2371–2378, (2004).

[16] H. Eisele, "480 GHz oscillator with an InP Gunn device," *Electron. Lett.*, 41(6), 422–423, (2010).

[17] E. Schomburg, J. Grenzer, K. Hofbeck, T. Blomeier, S. Winnerl, S. Brandl, A. A. Ignatov, K. F. Renk, D. G. Pavel'ev, Yu. Koschurinov, V. Ustinov, A. Zhukov, A. Kovsch, S. Ivanov, and P. S. Kop'ev, "Millimeter wave generation with a quasi planar superlattice electronic device," *Solid-State Electron.*, 42, (7–8), 1495–1498, (1998).

[18] H. Eisele, "355 GHz oscillator with GaAs TUNNETT diode," *Electron. Lett.*, 41(6), 329–331, (2005).

[19] H. Eisele, "Third-harmonic power extraction from InP Gunn devices up to 455 GHz," *IEEE Microw. Wireless Compon. Lett.*, 19(6), 416–418, (2009).